Fractional wettability effects on two-and three-fluid capillary pressure–saturation relations

Scott A. Bradford, Feike J. Leij *

U.S. Salinity Laboratory, U.S. Department of Agriculture, Agricultural Research Service, 450 Big Springs Road, Riverside, CA 92507, USA

Abstract

Studies of the relation between capillary pressure (P_c) and fluid saturation (S) for porous media containing oil–water or air–oil–water, often assume that the medium is strongly water-wet. Natural porous media, however, are composed of a variety of mineral constituents; such media are typically composed of water- and oil-wet fractions. This study reports on two- and three-fluid $P_c–S$ data for media of different fractions of water- and oil-wet sands. The oil–water capillary pressure, defined as the oil minus the water pressure, was measured during drainage (primary and main curves) as well as imbibition (main curve only) of water. A decrease in oil–water pressure was observed as the oil-wet fraction increased in two-fluid media. The pressure became negative during imbibition of water for relatively oil-wet media. The $P_c–S$ data could be adequately described by modifying the van Genuchten model for water retention. The observed differences between primary and main drainage curves were partly attributed to the effect of initial saturation. In three-fluid systems with fractional wettability, the observed dependency of capillary pressures on fluid saturations suggested that there was no continuous intermediate phase —even for a relatively low oil-wet fraction (25%). The oil–water and air–water capillary pressures decreased, at a particular water saturation, as the fraction of oil-wet sand increased. The water pressure is greater when water acts as the intermediate fluid than when it is the wetting fluid. The oil pressure, and hence the air–oil capillary pressure, was relatively insensitive to whether oil acted as wetting or intermediate fluid. There is a need to model three-fluid $P_c–S$ curves that account for different wetting and intermediate fluids.

---

* Corresponding author.

1. Introduction

Multiphase flow models require knowledge of the capillary pressure (P_c)–saturation (S) relations to accurately predict the spatial and temporal distributions of immiscible organic contaminants. The experimental determination of two-liquid and three-fluid P_c–S relationships is cumbersome. These relationships are frequently predicted from more widely available P_c–S data for air–water systems (Leverett, 1941; Demond and Roberts, 1991). Scaling approaches and empirical models of P_c–S relations assume that the medium is strongly wetted by only one of the liquids in two-liquid systems (Lenhard and Parker, 1988; van Genuchten, 1980). For three-fluid systems it is also assumed that the intermediate fluid (I) forms a continuous layer between the wetting (W) and nonwetting (N) fluids (Leverett, 1941; Lenhard and Parker, 1988). These assumptions may not necessarily be true for most natural porous media.

Wettability refers to the tendency of one fluid to spread on or adhere to a solid (s) surface in the presence of immiscible fluids (Craig, 1971). In natural porous media, the wettability varies from point to point depending upon the surface roughness (Morrow, 1976), immobile adsorbed liquid layers (Adamson, 1990, p.395) and the adsorptive properties of the mineral constituents. W.G. Anderson (1987) reported that coal, graphite, sulfur, talc, talc-like silicates, and many sulfides are probably neutrally wet to oil-wet. On the other hand, most common aquifer materials —such as quartz, carbonates and sulfates — are strongly water-wet. The wettability of originally water-wet porous media can be altered by adsorption of polar compounds and/or the deposition of organic material (Powers and Tambin, 1993; Demond et al., 1994). Consequently, many natural porous media containing oil (o) and water (w) have a fractional wettability; water adheres to water-wet solids whereas oil adheres to oil-wet solids. The fractional or mixed wettability of porous media has been recognized as a ubiquitous condition in the petroleum literature (Brown and Fatt, 1956; Iwankow, 1960; Gimatudinov, 1963). Fractional wettability refers to the fraction of the total pore surface area which is preferentially water- or oil-wet (Brown and Fatt, 1956). Salathiel (1973) introduced the term mixed wettability for the special case where oil-wet surfaces form continuous paths in the larger pores.

The fractional wettability of natural porous media has largely been ignored in hydrology and soil science, where researchers have primarily dealt with air–water systems. The large difference in density between water and air (a) facilitates the wetting of the solid by water. However, water-repellant soils are commonly encountered (Letey et al., 1975). Water repellency has been attributed to a variety of hydrophobic materials in soils, including fungal hyphae, humic acids and decomposing plant matter (Dekker and Ritsema, 1994). Contact angles, as measured by putting a drop of water on a flat solid, are much lower in the presence of air than in the presence of an oil (Wei et al., 1993). This suggests that fractional wettability is more prevalent than water repellency.

A second reason why fractional wettability may not have been widely reported is due to experimental methodology. Oil–water P_c–S curves are often obtained in a similar fashion as air–water P_c–S curves. An initially water-saturated soil column is placed on a hydrophilic end plate; an oil pressure is imposed at the top such that oil will enter/exit at the top while water flows through the plate at the bottom (cf. Demond and Roberts,

1991). Experimental values for S are only observed for the region of the P_c–S curve where the water pressure is less than the oil pressure.

Limited information is available on the influence of fractional wettability on P_c–S curves. Fatt and Klikoff (1959) measured P_c–S relations for water drainage in oil–water sandpacks consisting of different mixtures of water-and oil-wet sands. They found that the fraction of oil-wet sand and its particle size were important for the P_c–S relationships. The rate of water imbibition has been found to rapidly decrease as the fraction of oil-wet grains increases (Gimatudinov, 1963). To our knowledge, no three-fluid P_c–S measurements have been made for porous media with fractional wettability. Recently, Bradford and Leij (1995) measured three-fluid P_c–S relations in oil-wet media and found that the intermediate water did not spread on the air–oil interface to form a continuous layer; existing methods to predict the corresponding capillary pressures as a function of oil or water saturation were inadequate. If the intermediate fluid is also discontinuous for media with fractional wettability our ability to predict and model the three-fluid P_c–S curves may similarly be limited.

The objective of this paper is to report on the measurement of two-and three-fluid P_c–S relations using air, oil and water as fluids in fractional wettability media. The P_c–S model of van Genuchten (1980) will be adapted to describe two-fluid P_c–S curves for negative and positive capillary pressures, as observed in media with fractional wettability.

1.1. Capillarity and wettability

The capillary pressure, i.e. the pressure drop over a fluid–fluid interface, is defined as the difference between the nonwetting and wetting fluid pressures. The definition of capillary pressure is more ambiguous when both water-and oil-wet sites are present. The oil–water capillary pressure is generally defined as $P_{ow} = P_o - P_w$, with water as the reference "wetting" fluid (W.G. Anderson, 1987). Consequently, P_{ow} may be positive or negative in oil–water media with fractional wettability.

Fig. 1 shows the main water imbibition and drainage paths of a generic P_{ow}–S_w^{ow}
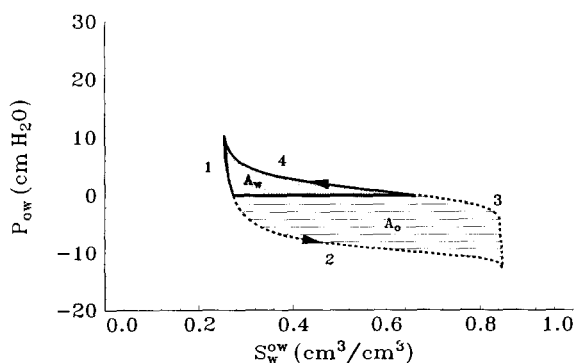

Fig. 1. Generic P_{ow}–S_w^{ow} relation and the areas, A_w and A_o, for determining I_{USBM}.

relation for a medium with fractional wettability. Saturations are expressed as fluid volume per unit pore volume; the subscript indicates the fluid to which the saturation pertains and the superscript denotes all fluids present in the medium. If the P_{ow}–S_w^{ow} curve is interpreted using the analogy with the rise of fluids in a capillary tube, water is the wetting fluid for $P_{ow} > 0$ and the nonwetting fluid for $P_{ow} < 0$. Consequently, the segments of the P_{ow}–S_w^{ow} curve labeled *1* and *4* correspond to the imbibition and drainage, respectively, of water from water-wet sites. Similarly, the segments labeled *2* and *3* reflect the drainage and imbibition, respectively, of oil from the oil-wet sites. Note that the capillary tube analogy is not always applicable; even strongly water-wet systems have a narrow range of saturations with $P_{ow} < 0$ due to the complex geometry of the porous medium (Purcell, 1950).

The wettability of a solid surface is typically characterized by the contact angle (ϕ), which is defined by a horizontal force balance at the contact line between a lighter fluid (l), a denser fluid (d) and a flat solid surface. Young's equation can be given as:

$$\cos(\phi_{sld}) = \frac{\sigma_{sl} - \sigma_{sd}}{\sigma_{ld}} \tag{1}$$

where σ is the interfacial tension (N m^{-1}); and the subscripts indicate the phases. The denser fluid wets the solid surface for $\phi_{sld} < 90°$, while the lighter fluid wets the solid surface for $\phi_{sld} > 90°$. The fluid that does not wet the solid is known as the nonwetting fluid. Different contact angles may occur when the wetting fluid is advancing (ϕ_{sld}^A) or receding (ϕ_{sld}^R). The equilibrium contact angle, ϕ_{sld}, corresponds to a unique free energy minimum; ϕ_{sld}^A and ϕ_{sld}^R are separated by energy barriers from the equilibrium value of ϕ_{sld} during metastable states (Hiemenz, 1986).

As noted earlier, the wettability is position dependent in many natural porous media. This is especially true in media with fractional wettability but also for homogeneous media due to variations in surface roughness. Consequently, the use of Eq. 1 to describe the wetting behavior of porous media has limited utility. Bradford and Leij (1995) used a curve fitting technique to determine the effective macroscopic advancing and receding contact angles, $\phi_{sld}^{A,R}$, from the relationship between capillary pressure and saturation for air and oil. It is assumed that $\phi_{sao}^{A,R} = 0°$ whereas the unknown contact angle is given by:

$$\phi_{sld}^{A,R} = \cos^{-1}\left(\frac{\sigma_{ao} P_{ld}(\bar{S}_d^{ld})}{\sigma_{ld} P_{ao}(\bar{S}_o^{ao})} \right) \tag{2}$$

where the effective saturation, $\bar{S}_d^{ld} = (S_d^{ld} - S_{rd}^{ld})/(1 - S_{rd}^{ld} - S_{rl}^{ld})$, maps $S_d^{ld} = S_{rd}^{ld}$ onto $\bar{S}_d^{ld} = 0$ and $S_d^{ld} = 1 - S_{rl}^{ld}$ onto $\bar{S}_d^{ld} = 1$; the subscript r denotes a residual value. Other effective saturations, $\bar{S}_o^{ao}$ and $\bar{S}_w^{ow}$, are similarly defined. A macroscopic value for ϕ_{sld}^A (imbibition) or ϕ_{sld}^R (drainage) was obtained according to Eq. 2 by fitting P_c–S data over a range in saturations. Since the contact angle is saturation dependent for media with fractional wettability, Eq. 2 was also used to scale individual points of the P_{ow}–S_w^{ow} and P_{ao}–S_o^{ao} curves to obtain a saturation-dependent contact angle, $\phi_{sow}(\bar{S}_w^{ow})$.

The average wettability of oil–water systems has also been quantified with the area under the P_{ow}–S_w^{ow} curve. The U.S. Bureau of Mines (USBM) method quantifies wettability using the principle that less work is necessary for displacing the nonwetting

by the wetting fluid than for the reverse displacement (Donaldson et al., 1969). The area under the drainage curves (cf. segments 2 and 4 of Fig. 1) corresponds to the external work per unit pore volume, W_{ext}, done to displace the wetting fluid. This work is defined as:

$$W_{ext} = -\int_{S_{iw}^{ow}}^{S_{w}^{ow}} P_{ow}(x)\,dx \tag{3}$$

where x is a dummy variable; and S_{iw}^{ow} is the initial saturation. The area under the imbibition curves (cf. segments 1 and 3 of Fig. 1) corresponds to the energy released during wetting of the solid (Hassanizadeh and Gray, 1993). Sharma and Wunderlich (1985) modified the approach by defining the water-wet area, A_w, for $P_{ow} > 0$ and the oil-wet area, A_o, for $P_{ow} < 0$. The ratio A_w/A_o provides an estimate of the fraction of water- and oil-wet solid surfaces. We will use the USBM wettability index, based on the modified areas, as defined by:

$$I_{USBM} = \log(A_w/A_o) \tag{4}$$

Note that $I_{USBM} = 0$ for equal fractions of water-and oil-wet solids ($A_w = A_o$).

In a three-fluid system, the wettability at the air–oil–water contact line is related to the coefficient of spreading for a drop of an intermediate (I) fluid on a wetting (W) fluid. This coefficient is defined as (Adamson, 1990, p. 110):

$$\Sigma_{I/W} = \sigma_{NW} - (\sigma_{NI} + \sigma_{IW}) \tag{5}$$

A negative value for $\Sigma_{I/W}$ indicates that the intermediate fluid does not spread on the wetting fluid, while a positive value suggests that the intermediate fluid will spread on the wetting fluid. Generally $\Sigma_{o/w}$ is positive for a water-wet medium and $\Sigma_{w/o}$ is negative for an oil-wet medium since $\sigma_{aw} > \sigma_{ao}$ for almost any oil.

2. Materials and methods

Porous media with fractional wettability were obtained by combining different portions of blasting sands that were untreated or treated with an organosilane. The sands were subsequently stirred to ensure a "uniform" fractional wettability medium. The untreated sands were strongly water-wet, while the organosilane treated sands were oil-wet in oil–water systems or water repellent in air–water systems. Air–water, oil–water and air–oil–water P_c–S relations were measured for sand mixtures composed of 0%, 25%, 50%, 75% and 100% treated sands. Air–oil P_c–S relations were only determined for 0% and 100% organosilane media. The treated media were obtained by adding blasting sand to a 5% solution of octadecyltrichlorosilane (OTS) in ethanol. The mixture was subsequently shaken for 5 h, after which the sand was air dried (R. Anderson et al., 1991).

For each P_c–S measurement, a column of known volume was filled with the initial wetting fluid-oil for the air–oil systems and water for all other cases — and packed with a predetermined mass of the blasting sand mixture to obtain a dry bulk density (ρ_b) of 1.71 g cm^{-3}. The porous medium consisted of several blasting sands: 12.6% each of ASTM sieve sizes #12 (1.8-mm diameter) and #16 (1.5 mm); 25.2% each of ASTM

sieve sizes #20 (0.9 mm) and #30 (0.6 mm); and 8.2% each of sizes ASTM sieve sizes #60 (0.25 mm), #70 (0.2 mm) and #90 (0.15 mm) [1]. This distribution corresponds to a mixture consisting of 25% very coarse sand, 50% coarse/medium sand and 25% fine sand according to the USDA textural classification (Soil Survey Staff, 1975). The porosity was calculated using a particle density of 2.65 g cm^{-3} (Danielson and Sutherland, 1986). The initial volume of the wetting fluid was assumed equal to the product of column volume and porosity.

The oil was Soltrol 220®, which is composed of a mixture of C_{13}–C_{17} hydrocarbons with a fluid density (ρ_o) of 0.8 g cm^{-3}. [2] The equilibrium interfacial tensions, measured with a du Noüy ring tensiometer (du Noüy, 1919), were $\sigma_{aw} = 0.072$ N m^{-1}, $\sigma_{ao} = 0.024$ N m^{-1} and $\sigma_{ow} = 0.026$ N m^{-1}. The measured value for the Soltrol®-contaminated air–water interface, σ_{aw}^*, was 0.052 N m^{-1}; the value of 0.072 N m^{-1} represents pristine conditions. It is realistic to use σ_{aw}^* since even a trace amount of oil can greatly affect σ_{aw} (Corey, 1986). Spreading coefficients are calculated according to Eq. 5; $\Sigma_{o/w} = 0.022$ N m^{-1} and $\Sigma_{w/o} = -0.074$ N m^{-1} if we use σ_{aw} whereas $\Sigma_{o/w}^* = 0.002$ N m^{-1} and $\Sigma_{w/o}^* = -0.054$ N m^{-1} if we use σ_{aw}^*.

Two-and three-fluid P_c–S relations were obtained according to the "Brooks method" by displacing a known quantity of fluid into or from the porous medium, and measuring the resulting fluid pressures until equilibrium is reached (Brooks and Corey, 1964). Liquid saturations were determined from a mass balance. The soil column consisted of two hydrophobic and two hydrophilic ring tensiometers; this allows for independent control of the saturation and monitoring of the pressure for both the water and oil phases. The design facilitates the fairly rapid measurement of P_c–S data; ~ 1 week was needed to measure the complete drainage and imbibition cycle in our case. If air was used as a fluid, the column was vented at the top through a pin hole to ensure that air in the medium is at atmospheric pressure. The automated measurement of the P_c–S relations, which is based upon the manual operation by Lenhard and Parker (1988), is described in Bradford and Leij (1995).

3. Results and discussion

3.1. Two-fluid systems

In this section the two-fluid P_c–S curves for air–oil, air–water and oil–water systems in mixtures of OTS and untreated sands are discussed. Particular attention is given to the effects of fractional wettability in oil–water systems. All capillary pressures are expressed as cm of water.

The primary drainage and main imbibition curves for air–oil media containing 0% and 100% OTS sand were presented earlier by Bradford and Leij (1995). The two P_{ao}–S_o^{ao} relations were found to be similar, indicating that Soltrol® strongly wets OTS

---

[1] Corona Industrial Sand Company, Corona, CA 91718, U.S.A.

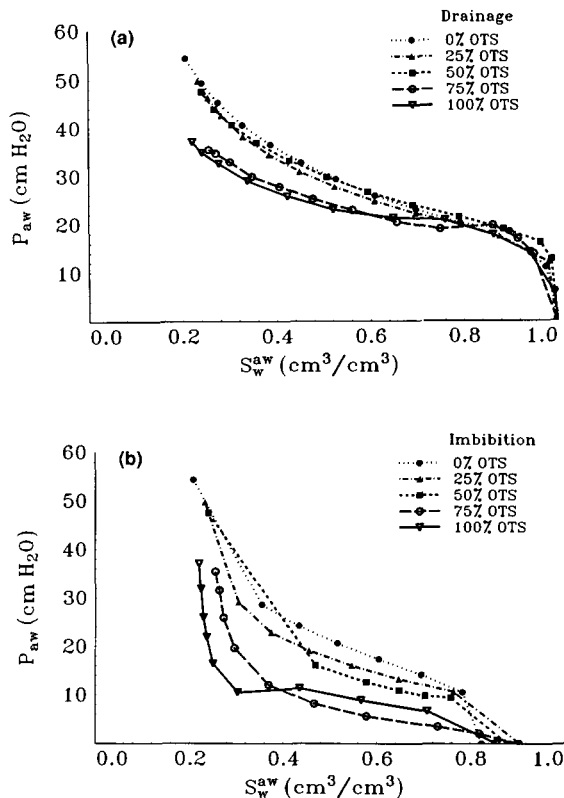[2] Phillips Petroleum Company, Bartlesville, OK 74004, U.S.A.

Fig. 2. Measured $P_{aw} - S_w^{aw}$ data for: (a) water drainage; and (b) water imbibition.

and untreated sands in comparison with air. This result is consistent with the low ϕ_{sao}, which follows from the low value for σ_{ao} of 0.024 N m^{-1}. The OTS fraction has little effect on the $P_{ao}-S_o^{ao}$ curves; no curves were obtained for the 25%, 50% and 75% OTS media.

Fig. 2a shows the P_c-S curves during primary drainage of water for air–water media consisting of 0%, 25%, 50%, 75% and 100% OTS sand. The curves for the 0%, 25% and 50% media are similar, as are the curves for the 75% and 100% OTS media. The more hydrophobic 75% and 100% OTS media have a lower P_{aw} at a given S_w^{aw}; it is relatively easy for water to be displaced by air. Fig. 2b shows the $P_{aw}-S_w^{aw}$ curves for water imbibition. The area under the imbibition branch decreases as the hydrophobicity increases (except for the 100% OTS medium). This suggests that a decreasing amount of energy is released during wetting of the solid by water (Hassanizadeh and Gray, 1993). The advancing and receding air–water contact angles, $\phi_{saw}^{A,R}$, obtained according to Eq. 2, are shown in Table 1. The general trend of an increase in ϕ_{saw}^{A} with the OTS fraction reflects the greater hydrophobicity. The value of P_{aw} is always greater than zero since the water pressure is measured with respect to atmospheric pressure, the fitted ϕ_{saw} are

Table 1
Fitted advancing and receding air–water contact angles

% OTS	ϕ_{saw}^{A} (°)	ϕ_{saw}^{R} (°)
0	0.00	0.00
25	40.6	28.0
50	51.2	21.5
75	72.7	38.4
100	64.9	38.0

hence always $< 90°$. Note that ϕ_{saw}^{R} is lower than ϕ_{saw}^{A}; the drainage curve is insensitive to changes in the contact angle (Morrow, 1975).

Fig. 3a shows the $P_{ow}-S_{w}^{ow}$ curves during primary water drainage in oil–water media with 0%, 25%, 50%, 75% and 100% OTS sand. The 0%, 25% and 50% OTS media $P_{ow}-S_{w}^{ow}$ curves are similar since wettability does not greatly affect drainage (Morrow, 1975). The area under the curve decreases as the fraction of OTS sand increases —less
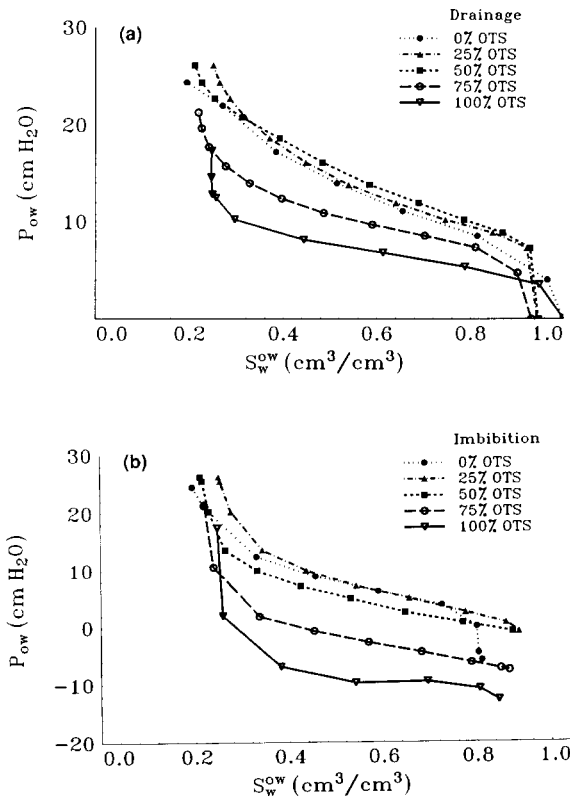

Fig. 3. Measured $P_{ow}-S_{w}^{ow}$ data for: (a) water drainage; and (b) water imbibition.

work is required to displace water by oil. Similarly, Fig. 3b shows the $P_{ow}-S_w^{ow}$ curves for water imbibition. The 0% and 25% OTS media have similar $P_{ow}-S_w^{ow}$ curves. Note that P_{ow} decreases as the fraction of OTS sand increases for a particular S_w^{ow}. The negative P_{ow}-values indicate forced water imbibition; water can only displace oil when a positive pressure is exerted on oil relative to water. The S_w^{ow}-value at which $P_{ow} = 0$ tends to decrease ($S_w^{ow} = 0.80$ for 0% OTS; $S_w^{ow} = 0.88$ for 25% OTS; $S_w^{ow} = 0.69$ for 50% OTS; $S_w^{ow} = 0.42$ for 75% OTS; and $S_w^{ow} = 0.27$ for 100% OTS) as the fraction of oil-wet sand increases. There is apparently a larger region with forced imbibition as the OTS fraction increases.

Empirical models of P_c-S relations, such as those of Brooks and Corey (1964) and van Genuchten (1980), are commonly employed to describe oil–water P_c-S curves. These models are better suited to describe P_c-S curves for air–liquid than two-liquid systems since they only consider positive capillary pressures. The van Genuchten model is written as:

$$P_{ow} = \frac{1}{\alpha}\left[\left(S_w^{ow}\right)^{n/(1-n)} - 1\right]^{1/n} \tag{6}$$

where n and α are empirical parameters. The model of van Genuchten was modified, to account for both positive and negative capillary pressures, according to:

$$P_{ow} + \gamma = \frac{1}{\alpha}\left[\left(\bar{S}_w^{ow}\right)^{n/(1-n)} - 1\right]^{1/n} \tag{7}$$

The parameter γ was set equal to the magnitude of the lowest observed P_{ow}; $P_{ow} + \gamma$ is therefore always ≥ 0. The conventional P_c-S model of van Genuchten was then used to describe the observed $(P_{ow} + \gamma)-\bar{S}_w^{ow}$ relation.

Table 2 shows relevant parameters for describing $P_{ow}-S_w^{ow}$ data obtained for the primary and main drainage, and the main imbibition curves of water. The use of the terms primary (or initial) and main is according to Klute (1986). Values for S_{rw}^{ow}, S_{ro}^{ow} and γ follow directly from the observations. Note that S_{ro}^{ow} and γ were set equal to zero during primary drainage. The residual saturations (S_{rw}^{ow} and S_{ro}^{ow}) correspond to the

Table 2
Parameters in the model according to Eq. 7 for describing $P_{ow}-\bar{S}_w^{ow}$ data for primary (PD)[†] and main (MD) water drainage and main water imbibition (MI)

% OTS	S_{rw}^{ow}	S_{ro}^{ow}	γ (cm)	α_{PD} (cm^{-1})	α_{MI} (cm^{-1})	α_{MD} (cm^{-1})	n	R
0	0.194	0.190	5.900	0.0874	0.0772	0.0563	5.0928	0.991
25	0.251	0.110	0.930	0.0939	0.1519	0.1035	3.8230	0.984
50	0.212	0.123	3.340	0.1023	0.2028	0.1153	3.8528	0.980
75	0.220	0.131	7.642	0.1169	0.2065	0.0949	4.5039	0.974
100	0.248	0.152	12.78	0.1606	0.3020	0.0783	5.6409	0.965

Values for S_{rw}^{ow}, S_{ro}^{ow} and γ are measured while α and n are fitted (R is the coefficient of correlation between fitted and observed data).
[†] S_{ro}^{ow} and γ are set to zero during primary drainage
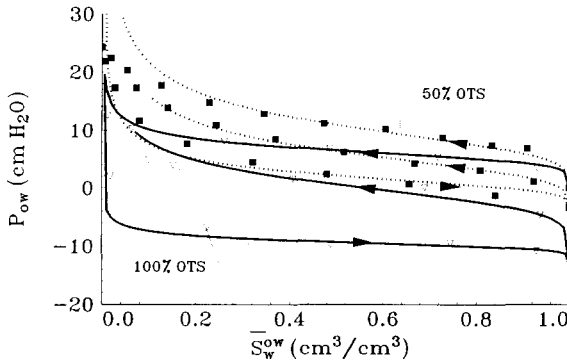
Fig. 4. Observed and fitted hysteretic $P_{ow} - \bar{S}_w^{ow}$ relations for the 50% and 100% OTS media.

lowest saturation attained during the experiments. Table 2 also shows α_{PD} (primary drainage), α_{MI} (main imbibition), α_{MD} (main drainage) and n (same for all three curves) obtained by fitting Eq. 7 to the $P_{ow} - \bar{S}_w^{ow}$ data. Note that α is inversely related to the bubbling or entry pressure while n depends on the slope at the inflection point of the $(P_{ow} + \gamma) - \bar{S}_w^{ow}$ relationship. Hence α and n depend on γ. The parameter optimization was done according to Marquardt (1963), the regression coefficient (R) was > 0.965 in all cases.

Fig. 4 shows the observed and fitted $P_{ow} - \bar{S}_w^{ow}$ relationships for the 50% and 100% OTS media (primary and main drainage, and main imbibition). The $P_{ow} - \bar{S}_w^{ow}$ relation is described reasonably well by Eq. 7. The difference between the primary and main drainage curves is greater for the more hydrophobic 100% OTS medium than the 50% OTS medium. The main drainage curve always has a lower P_{ow} than the primary drainage curve for a given $\bar{S}_w^{ow}$. Differences between the primary and main drainage curves are typically attributed to entrapment of the nonwetting fluid (cf. Stonestrom and Rubin, 1989). This explanation may not adequately explain the observed differences, as we will discuss below.

Fig. 5 shows the hysteretic $\phi_{sow}(S_w^{ow})$ curves for the 100% OTS medium as calculated according to Eq. 2 for individual $P_{ow} - S_w^{ow}$ data. The value of ϕ_{sow} depends on the saturation history. The $\phi_{sow}(S_w^{ow})$-value during primary drainage is below the curve for main drainage. Note that ϕ_{sow} is independent of saturation for primary drainage. In contrast, ϕ_{sow} depends on saturation during main imbibition and drainage. Apparently, water hinders oil from wetting the OTS sand during primary drainage; a relatively high P_{ow} is required for oil to displace water (cf. Fig. 4). During the subsequent (main) drainage cycle, after oil has already penetrated water films to wet the OTS sand, oil displaces water at a lower P_{ow}. A similar phenomenon contributed to the observed differences between the primary and main drainage $P_{ow} - S_w^{ow}$ curves for the other fractional wettability media.

The wettability of media containing oil and water was also quantified with the USBM wettability index, I_{USBM} (cf. eq. 4). Fig. 6 shows the calculated I_{USBM} as a function of the fraction of OTS sand. The values were determined from A_w and A_o according to
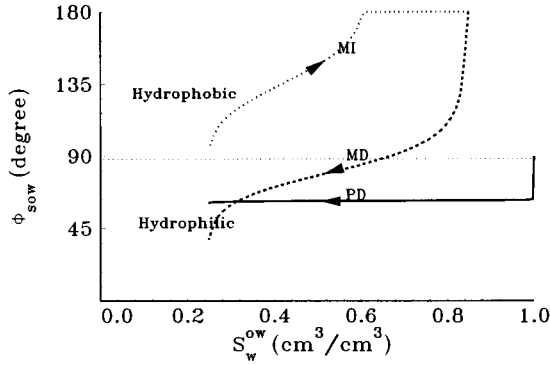
Fig. 5. Values of $\phi_{sow}(S_w^{ow})$ calculated according to Eq. 2 from $P_{ow}-S_w^{ow}$ data for 100% OTS media.

Eq. 3 using numerical integration of the modified van Genuchten $P_{ow}-\bar{S}_w^{ow}$ model. The fitted model parameters shown in Table 2 were used for a continuous description of the $P_{ow}-\bar{S}_w^{ow}$ data. Two values were calculated: (1) I_{USBM}^1, which uses parameters from the primary drainage (A_w for $P_{ow} > 0$) and main imbibition (A_o for $P_{ow} < 0$) curves; and (2) I_{USBM}^2, calculated with model parameters from the main drainage and imbibition curves. Note that I_{USBM} can be positive even when the medium contains a substantial fraction (up to 75%) of the hydrophobic OTS sand. For all media I_{USBM}^1 exceeds I_{USBM}^2, the difference increases with the OTS fraction. This result can also be partly attributed to the difference in initial fluid saturation.

Linear regression of the data in Fig. 6 yielded the following relationships:

$$I_{USBM}^1 = -0.0306 \cdot \%OTS + 2.925 \qquad (R = 0.992) \tag{8}$$

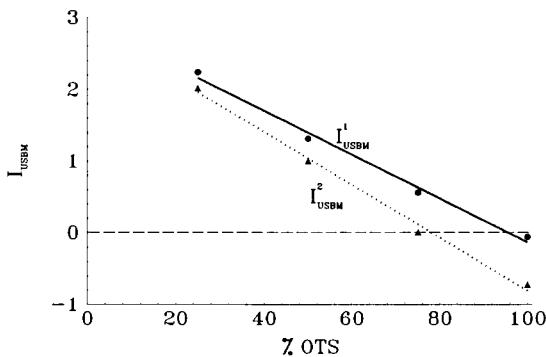$$I_{USBM}^2 = -0.03684 \cdot \%OTS + 2.88 \qquad (R = 0.994) \tag{9}$$

Fig. 6. USBM wettability indices, I_{USBM}, determined from $P_{ow}-\bar{S}_w^{ow}$ data as a function of the OTS fraction (I_{USBM}^1 and I_{USBM}^2 are calculated from a primary and main drainage curve, respectively, and the main imbibition curve).

In case P_{ow}–S_w^{ow} data are available for another medium with fractional wettability, an initial estimate of the oil-wet fraction of that medium may be obtained with Eq. 8 or Eq. 9. Unfortunately, the P_c–S measurements were conducted over a fairly narrow range of pressures to ensure that the entry pressures of the hydrophilic and hydrophobic ceramics, which form the ring tensiometers, were not exceeded. Consequently, the values for S_{rw}^{ow} and S_{ro}^{ow}, which are the end points of each cycle, are relatively high (cf. Table 2). This may introduce a bias in our calculated I_{USBM}-values.

3.2. Three-fluid systems

This section deals with P_c–S curves of media containing air, oil and water. We are again interested in the effect of fractional wettability (25%, 50% and 75% OTS) on three-fluid P_c–S relationships. Three-fluid systems were obtained by incrementally adding oil to a medium containing air and a fixed amount of water. Subsequently, various drainage and imbibition paths were followed to achieve a wide range of oil,
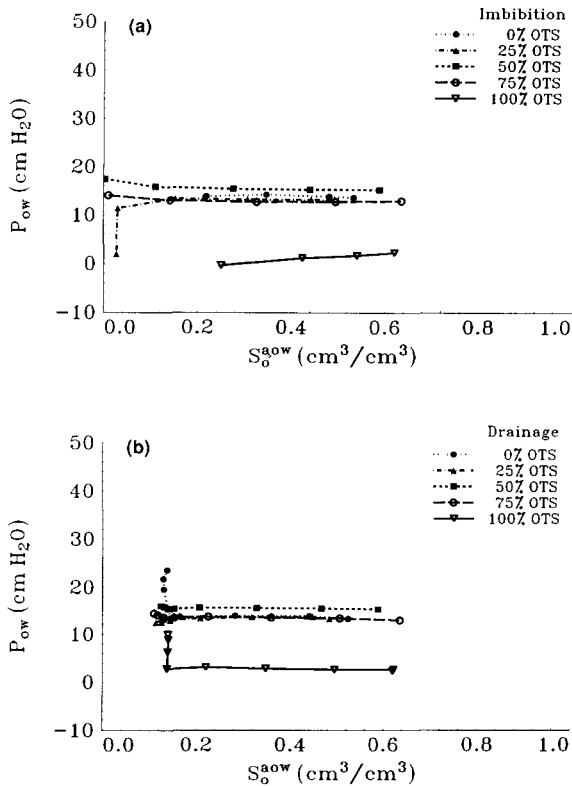

Fig. 7. Measured P_{ow}–S_o^{aow} data for: (a) oil imbibition; and (b) oil drainage. The water saturation is constant ($S_w^{aow} = 0.27$ for 0% OTS, $S_w^{aow} = 0.44$ for 25% OTS, $S_w^{aow} = 0.28$ for 50% OTS, $S_w^{aow} = 0.25$ for 75% OTS, $S_w^{aow} = 0.27$ for 100% OTS).

water and air saturations. Four different types of measurements can be distinguished: (1) oil imbibition (at constant S_w^{aow}); (2) oil drainage (at constant S_w^{aow}); (3) water imbibition (at constant S_0^{aow}); and (4) water drainage (at constant S_0^{aow}).

Results for hydrophilic (0% OTS) and hydrophobic (100% OTS) media were presented earlier by Bradford and Leij (1995). It was observed that P_{ow} depends on S_w^{aow} while P_{ao} is uniquely determined by S_{tl}^{aow} for the 0% OTS medium. Apparently oil forms a continuous intermediate oil phase; the positive spreading coefficient ($\Sigma_{o/w}^* = 0.002$ N m^{-1}) suggests that oil will spread on the air–water interface. In contrast, the behavior of P_c–S curves is more complicated for the 100% OTS medium. The values of P_{ow} and P_{aw} were mainly functions of S_w^{aow}, while P_{ao} was mainly a function of S_0^{aow}. It is not likely that water forms a continuous intermediate layer since it does not spread well on the air–oil interface ($\Sigma_{w/o}^* = -0.054$ N m^{-1}). Wettability may greatly affect capillary pressure curves of three-fluid systems due to its effect on the intermediate fluid.

Fig. 7 shows P_{ow}–S_0^{aow} curves for three-fluid media with 0%, 25%, 50%, 75% and 100% OTS sand, at constant water saturation, for: (a) imbibition of oil and (b) drainage
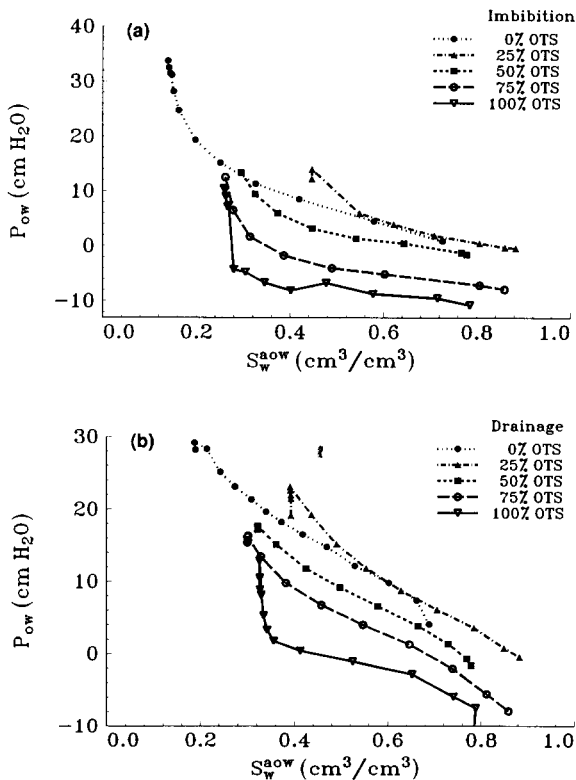

Fig. 8. Measured P_{ow}–S_w^{aow} data for: (a) water imbibition; and (b) water drainage. The oil saturation is constant ($S_0^{aow} = 0.14$ for 0% OTS, $S_0^{aow} = 0.13$ for 25% OTS, $S_0^{aow} = 0.12$ for 50% OTS, $S_0^{aow} = 0.11$ for 75% OTS, $S_0^{aow} = 0.15$ for 100% OTS).

of oil. Fig. 8, on the other hand, shows $P_{ow}-S_w^{aow}$ curves when the oil saturation is kept constant for: (a) imbibition of water and (b) drainage of water. A comparison between the curves, for different OTS fractions, in Fig. 7 and Fig. 8 shows that P_{ow} depends on S_w^{aow} but not on S_o^{aow}. Notice in Fig. 8 that, just as for two-fluid media (Fig. 3), P_{ow} decreases with increasing OTS fraction. Furthermore, P_{ow} is always positive for the 25% and 50% OTS media. In contrast, P_{ow} is almost exclusively negative during water imbibition of the 75% and 100% OTS media, i.e. for S_w^{aow} greater than 0.35 and 0.28, respectively; while it is negative during water drainage if $S_w^{aow} > 0.69$ for 75% OTS and already for $S_w^{aow} > 0.43$ for 100% OTS. A negative capillary pressure implies that water acts mainly as intermediate fluid.

Fig. 9 illustrates the behavior of the capillary pressure across the air–oil interface as a function of total liquid saturation (i.e. $P_{ao}-S_{tl}^{aow}$) at constant water saturation for: (a) oil imbibition and (b) oil drainage. Fig. 10 contains curves for the same variables but now for constant oil saturation and: (a) water imbibition and (b) water drainage. A comparison of Fig. 9a with Fig. 10a and of Fig. 9b with Fig. 10b reveals that P_{ao} is slightly
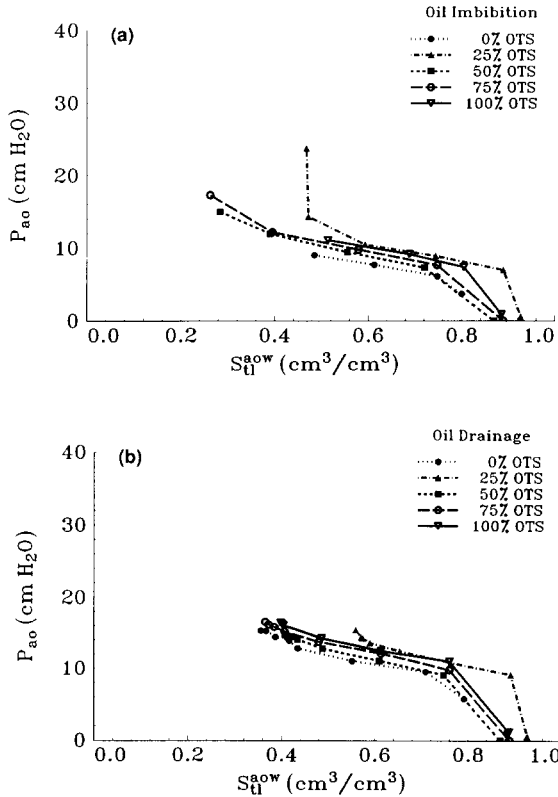
Fig. 9. Measured $P_{ao}-S_{tl}^{aow}$ data for: (a) oil imbibition; and (b) oil drainage. The water saturation is constant ($S_w^{aow} = 0.27$ for 0% OTS, $S_w^{aow} = 0.44$ for 25% OTS, $S_w^{aow} = 0.28$ for 50% OTS, $S_w^{aow} = 0.25$ for 75% OTS, $S_w^{aow} = 0.27$ for 100% OTS).
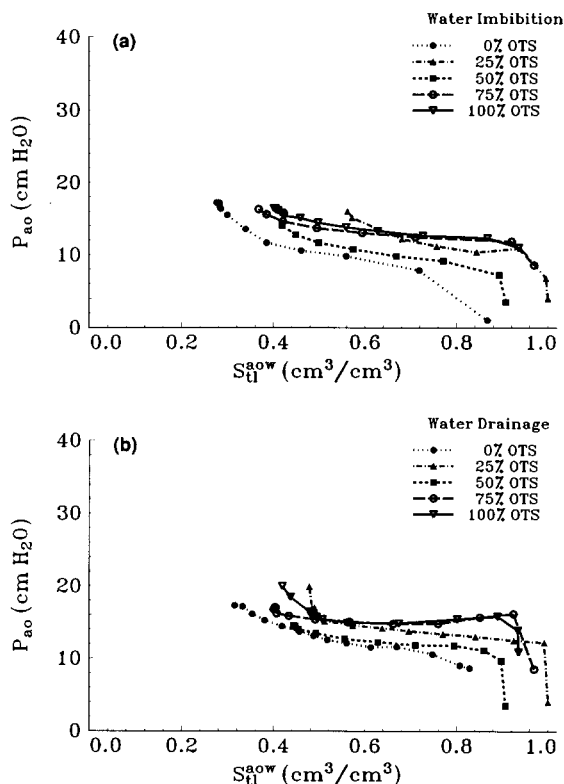
Fig. 10. Measured $P_{ao}-S_{tl}^{aow}$ data for: (a) water imbibition; and (b) water drainage. The oil saturation is constant ($S_o^{aow} = 0.14$ for 0% OTS, $S_o^{aow} = 0.13$ for 25% OTS, $S_o^{aow} = 0.12$ for 50% OTS, $S_o^{aow} = 0.11$ for 75% OTS, $S_o^{aow} = 0.15$ for 100% OTS).

more affected by changes in S_w^{aow} than by changes in S_o^{aow} for the 25%, 50%, 75% and 100% OTS fractions (especially during drainage Fig. 9b and 10b). Note that the OTS fraction has little influence on the $P_{ao}-S_{tl}^{aow}$ curves when S_o^{aow} is varied (Fig. 9). The initial oil saturation, which depends on the OTS fraction, primarily influences P_{ao} when S_w^{aow} is varied (Fig. 10).

The remaining capillary pressure to be investigated concerns the air–water interface. Fig. 11 presents $P_{aw}-S_{tl}^{aow}$ curves involving constant water saturation for: (a) oil imbibition and (b) oil drainage. Fig. 12 pertains to the same relationship when the oil saturation is constant for: (a) water imbibition and (b) water drainage. The results for the 0% OTS medium are not shown since no air–water interfaces are believed to exist (Bradford and Leij, 1995). It appears that P_{aw} is more affected by changes in S_w^{aow} (Fig. 12) than by changes in S_o^{aow} (Fig. 11). In both cases P_{aw} decreases, at a given S_{tl}^{aow}, for an increasing OTS fraction. The effect of wettability on P_{aw} is more pronounced for a variable water than oil saturation.

The results for three-fluid media indicate that the capillary pressures in fractional wettability systems (25%, 50% and 75% OTS) behave in a similar manner as for the
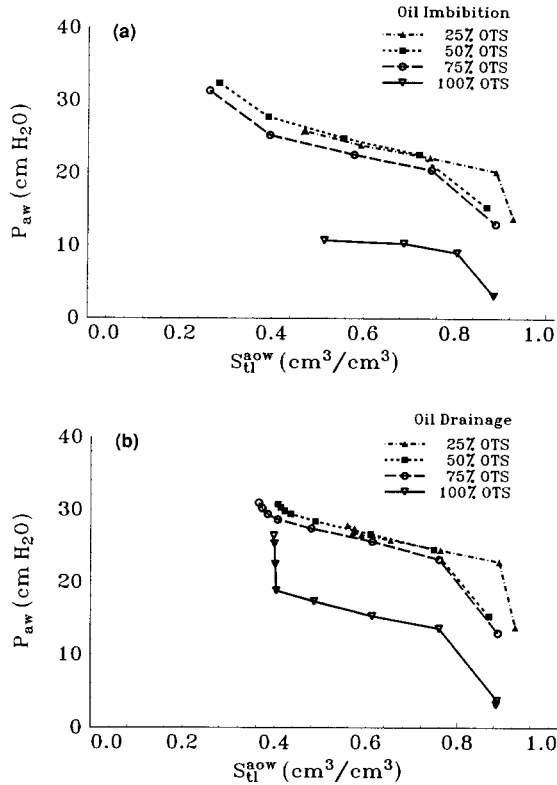
Fig. 11. Measured $P_{aw} - S_{tl}^{aow}$ data for: (a) oil imbibition; and (b) oil drainage. The water saturation is constant ($S_w^{aow} = 0.44$ for 25% OTS, $S_w^{aow} = 0.28$ for 50% OTS, $S_w^{aow} = 0.25$ for 75% OTS, $S_w^{aow} = 0.27$ for 100% OTS).

100% OTS medium; P_{ow} and P_{aw} are mainly functions of S_w^{aow}, while P_{ao} is mainly a function of S_o^{aow}. Neither P_{ao} (Fig. 9 and Fig. 10) nor P_{aw} (Fig. 11 and Fig. 12) are unique functions of S_{tl}^{aow}. Such unique dependency is expected if the intermediate fluid were to form a continuous layer (Leverett, 1941). It is therefore unlikely that the intermediate layer is continuous for the 25%, 50%, 75% and 100% OTS media. The reason for the discontinuity is that different fractions of the porous medium are water- and oil-wet, the intermediate fluids associated with these fractions, are presumably oil and water, respectively. Since water does not spread on the air–oil interface, there may also be some air–oil interfaces near oil-wet sites.

Changes in S_w^{aow} and S_o^{aow} both affect the air saturation; we postulate that the changes will primarily occur at the air–water and air–oil interfaces, respectively. As previously mentioned, such interfaces are present in our fractional wettability media. Consequently, P_{aw} is mainly a function of S_w^{aow} (cf. Fig. 12) while P_{ao} mainly depends on S_o^{aow} (cf. Fig. 9).

A change in S_w^{aow}, at a constant S_o^{aow}, will alter P_{ow} regardless whether water is the intermediate or wetting fluid (cf. Fig. 8). If water is the wetting fluid, a change in S_w^{aow}
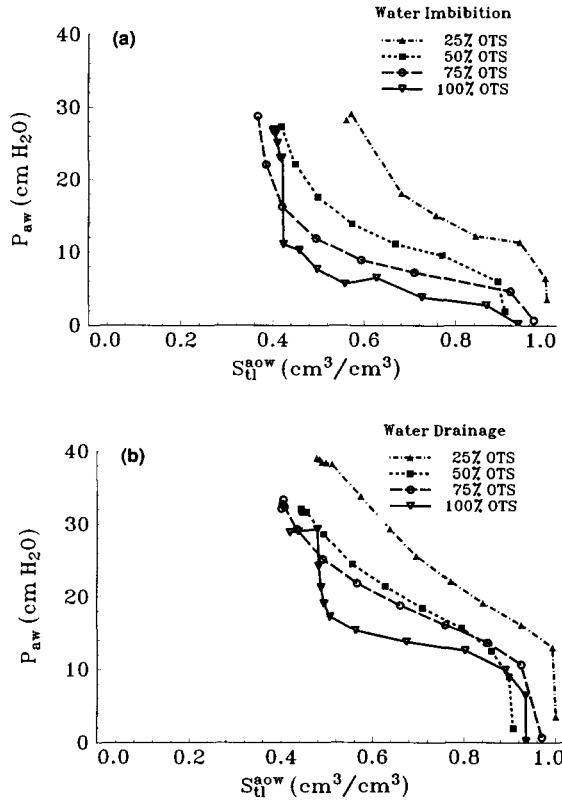
Fig. 12. Measured $P_{aw} - S_{tl}^{aow}$ data for: (a) water imbibition; and (b) water drainage. The oil saturation is constant ($S_o^{aow} = 0.13$ for 25% OTS, $S_o^{aow} = 0.12$ for 50% OTS, $S_o^{aow} = 0.11$ for 75% OTS, $S_o^{aow} = 0.15$ for 100% OTS).

will move the oil–water interface since the intermediate oil spreads well; this interface will hardly be affected if S_o^{aow} is varied. If water is the intermediate fluid, it does not spread well and the wetting fluid (oil) will be in contact with both air and water. Any change in water and air saturation will lead to a different fluid configuration at the oil surface; P_{ow} will also change with S_w^{aow} if water is the intermediate fluid. In contrast, a change in S_o^{aow} and S_a^{aow} will affect the air–oil interface (cf. Fig. 9), the oil–water interface is not likely to change much since S_w^{aow} is constant (cf. Fig. 7). Hence, P_{ow} is relatively unaffected by changes in oil saturation, regardless of oil being the wetting or intermediate fluid.

An increase in OTS fraction (hydrophobicity) will lower the $P_{ow} - S_w^{aow}$ (Fig. 8) and $P_{aw} - S_{tl}^{aow}$ (Fig. 12) curves when the water saturation is varied. This effect is due to differences in the wetting/spreading behavior of water near water-and oil-wet solids. These differences follow directly from the values of the contact angle and coefficient of spreading. The contact angles for the 0% OTS oil–water media were $\phi_{sow}^R = 0°$ and $\phi_{sow}^A = 51.6°$; these values were obtained by curve fitting according to Eq. 2. We already

noted that $\Sigma_{w/o}^{*} = -0.054$ N m^{-1}. The affinity of the untreated sand for water is apparently much stronger than the affinity of oil for water. As the OTS fraction increases, intermediate water near oil-wet solids may be replaced by air at lower P_{aw} or P_{ow}. The P_{ao}–S_{tl}^{aow} curves are not greatly affected by changes in S_{w}^{aow} (Fig. 10); the P_{ao}-value is mostly determined by the (constant) oil saturation.

When S_{0}^{aow} is varied for a constant S_{w}^{aow}, the P_{ao}-value at a given S_{tl}^{aow} is fairly insensitive to the OTS fraction (Fig. 9). This can again be explained with the spreading and wetting behavior of oil. Oil wets the OTS treated solid well since $\phi_{sao}^{A,R} = 0°$ (Bradford and Leij, 1995), while oil also spreads on water if it is the intermediate fluid ($\Sigma_{o/w}^{*} = 0.002$ N m^{-1}). Consequently, it is immaterial for the value of P_{ao} whether oil acts as the wetting or intermediate fluid. As noted earlier, P_{ow} (Fig. 7) and P_{aw} (Fig. 11) are not affected much by changes in S_{0}^{aow}; their values are primarily determined by the constant water saturation.

4. Summary and conclusions

The influence of fractional wettability on two-and three-fluid P_c–S relations was investigated for air–water, oil–water and air–oil–water media. Media with fractional wettability were obtained by combining different portions of untreated and OTS-treated blasting sands. The untreated sands were strongly water-wet, while the OTS sands were oil-wet in two-liquid systems or water repellent in air–water systems. Two-and three-fluid P_c–S relations were obtained for media with an OTS fraction of 0%, 25%, 50%, 75% and 100%.

In air–water systems the area under the drainage and imbibition P_{aw}–S_{w}^{aw} curves decreased as the OTS fraction (i.e. hydrophobicity) increased. The water drainage curve was less sensitive to these wettability effects than the imbibition curve.

Values of P_{ow}, defined as P_0–P_w, can be positive or negative in these fractional wettability media. The P_{ow}-value for a given S_{w}^{ow} decreased as the OTS fraction increased since less work is required for oil to displace water. An increase in OTS fraction also causes the saturation (S_{w}^{ow}) at which $P_{ow} = 0$ to decrease, i.e. the forced imbibition region expands.

The experimental P_{ow}–S_{w}^{ow} curves were quite different for primary and main drainage of water. The main drainage curve has a lower P_{ow}, for a given S_{w}^{ow}. The difference increased with hydrophobicity (OTS fraction). The values for the contact angle, ϕ_{sow}, for the 100% OTS fraction depended substantially more on saturation (S_{w}^{ow}) during main imbibition and drainage than during primary drainage. This suggests that the initial fluid saturation affected the P_{ow}–S_{w}^{ow} curve. We hypothesized that, during primary drainage, water posed a greater hindrance for oil to wet the OTS sand than during the subsequent main drainage. Conventional (empirical) models for P_c–S cannot readily be applied to describe P_c–S curves of two-fluid media with fractional wettability since they assume that the capillary pressure is always positive. The model of van Genuchten was in effect modified by adding a shifting parameter, γ, to the pressure values so that $P_{ow} + \gamma$ is always ≥ 0. The P_c–S model of van Genuchten was then used to describe the $(P_{ow} + \gamma)$–$\bar{S}_{w}^{ow}$ data. This model was successfully fitted to P_{ow}–S_{w}^{ow} data; the regression coefficients for the goodness of fit were always > 0.965.

A slightly modified form of the USBM wettability index, I_{USBM}, was determined from drainage and imbibition curves of oil–water systems. The index involving primary drainage was higher than the index obtained from main drainage data. This result was partly attributed to the aforementioned effect of the initial saturation. The values of I_{USBM} were positive even if the medium contains significant portions of OTS sand ($< 75\%$). A linear relationship between I_{USBM} and the OTS fraction was obtained by regression analysis. These relationships could be used to estimate the oil-wet fraction of other media with fractional wettability for which P_{ow}–$\overline{S}_w^{ow}$ data are available.

In three-fluid media with fractional wettability, the values of P_{ow} and P_{aw} were observed to mainly depended on S_w^{aow}, while values for P_{ao} were mainly a function of S_o^{aow}. There is apparently no continuous intermediate fluid in these media. The dependency of three-fluid capillary pressures on fluid saturations was explained by assuming that changes in S_w^{aow} and S_o^{aow}, which led to corresponding changes in S_a^{aow}, occurred primarily at the air–water and air–oil interfaces, respectively.

The OTS fraction affected the P_{ow}–S_w^{aow} and P_{aw}–S_{tl}^{aow} curves when S_w^{aow} was varied (constant S_o^{aow}). On the other hand, the OTS fraction was not important for the P_{ao}–S_{tl}^{aow} curve when S_o^{aow} was varied (constant S_w^{aow}). These results were explained with the contrasting wetting/spreading behavior of water and oil. The untreated sand (water as wetting fluid) and oil (water as intermediate fluid) had different affinities to water. Consequently, the values of P_{ow} and P_{aw} will be affected by the role of water; the OTS fraction determines how much water act as intermediate and wetting fluid. On the other hand, the OTS sand (oil as wetting fluid) and water (oil as intermediate fluid) have a similar affinity to oil; P_{ao} was therefore relatively unaffected by the OTS fraction. The P_{ow}–S_o^{aow} and P_{aw}–S_{tl}^{aow} curves for a variable S_o^{aow} are mostly determined by the value of the constant S_w^{aow}. Similarly, the P_{ao}–S_{tl}^{aow} curves were relatively unaffected by the OTS fraction when S_w^{aow} was varied at constant oil saturation.

5. Notation

a	air
A_o	area of P_{ow}–S_w^{ow} curve with $P_{ow} < 0$ (N m^{-2}, cm water)
A_w	area of P_{ow}–S_w^{ow} curve with $P_{ow} > 0$ (N m^{-2}, cm water)
d	denser fluid
I	intermediate wetting fluid
I_{USBM}^1	USBM wettability index for primary drainage and main imbibition
I_{USBM}^2	USBM wettability index for main drainage and imbibition
l	lighter fluid
n	parameter in van Genuchten model for P_c–S
N	nonwetting fluid
o	oil
OTS	octadecyltrichlorosilane
P_c	capillary pressure (N m^{-2}, cm water)
P_i	pressure of fluid i (N m^{-2}, cm water)
P_{ij}	pressure drop over interface between fluids i and j, i.e. $P_i - P_j$ (N m^{-2}, cm water)

s   solid
S saturation $(\text{cm}^3 \text{ cm}^{-3})$
$\bar{S}$ effective saturation, i.e. $(S_\text{W}^\text{NW} - S_\text{rW}^\text{NW})/(1 - S_\text{rW}^\text{NW} - S_\text{rN}^\text{NW})$
S_i^{ij} saturation of fluid i in a medium containing fluids i and j $(\text{cm}^3 \text{ cm}^{-3})$
S_i^{ijk} saturation of fluid i in a medium containing fluids i, j and k $(\text{cm}^3 \text{ cm}^{-3})$
S_iw^ow initial water saturation in an oil–water system $(\text{cm}^3 \text{ cm}^{-3})$
S_r residual saturation $(\text{cm}^3 \text{ cm}^{-3})$
S_tl^{ijk} total liquid saturation $(\text{cm}^3 \text{ cm}^{-3})$
w   water
W   wetting fluid
W_ext external work per unit pore volume (N m^{-2})
x dummy variable $(\text{cm}^3 \text{ cm}^{-3})$
α parameter in the van Genuchten model for P_c–S (1 cm^{-1})
γ shifting parameter in modified model for P_c–S (cm water)
ρ_b bulk density (g cm^{-3})
ρ_o density of oil (g cm^{-3})
$\Sigma_{i/j}$ coefficient for spreading of fluid i on fluid j (N m^{-1})
$\Sigma_{i/j}^*$ coefficient for spreading of contaminated fluid i on fluid j (N m^{-1})
σ_{ij} interfacial tension at interface between fluids i and j (N m^{-1})
σ_aw^* interfacial tension between air and contaminated water (N m^{-1})
ϕ_{sij} equilibrium contact angle at contact line between solid and fluids i and j $(°)$
ϕ_{sij}^A advancing contact angle $(°)$
ϕ_{sij}^R receding contact angle $(°)$

Acknowledgements

References

Adamson, A.W., 1990. Physical Chemistry of Surfaces. Wiley, New York, NY, 5th ed., 777 pp.

Anderson, R., Larson, G. and Smith, C., 1991. Silicon Compounds: Register and Review —5th Edition. Huls America Inc., Piscataway, NJ.

Anderson, W.G., 1987. Wettability literature survey —Part 4: Effects of wettability on capillary pressure. J. Pet. Technol., 1283–1299.

Bradford, S. and Leij, F.J., 1995. Wettability effects on scaling two-and three-fluid capillary pressure–saturation relations. Environ. Sci. Technol., 29: 1446–1455.

Brooks, R.H. and Corey, A.T., 1964. Hydraulic Properties of Porous Media. Colo. State Univ., Fort Collins, CO, Hydrol. Pap. No. 3.

Brown, R.J.S. and Fatt, I., 1956. Measurements of fractional wettability of oilfield rocks by the nuclear magnetic relaxation method. Trans. AIME (Am. Inst. Min. Metall. Eng.), 207: 262–264.

Corey, A.T., 1986. Mechanics of Immiscible Fluids in Porous Media. Water Resources Publications, Littleton, CO.

Craig, F.F., 1971. The Reservoir Engineering Aspects of Waterflooding. Soc. Pet. Eng., Richardson, TX, Monogr. Ser. No. 3.

Danielson, R.E. and Sutherland, P.L., 1986. Methods Soil Analysis, Part 1 —Physical and Mineralogical Methods —Second Edition, Ch. 18: Porosity. ASA–SSSA (Am. Soc. Agron.–Soil Sci. Soc. Am.), Madison, WI.

Dekker, L.W. and Ritsema, C.J., 1994. How water moves in a water repellent sandy soil, 1. Potential and actual water repellency. Water Resour. Res., 30: 2507–2519.

Demond, A.H. and Roberts, P.V., 1991. Effect of interfacial forces on two-phase capillary pressure–saturation relationships. Water Resour. Res., 27: 423–437.

Demond, A.H., Desai, F.N. and Hayes, K.F., 1994. Effect of cationic surfactants on organic liquid–water capillary pressure–saturation relationships. Water Resour. Res., 30: 333–342.

Donaldson, E.C., Thomas, R.D. and Lorenz, P.B., 1969. Wettability determination and its effect on recovery efficiency. Soc. Pet. Eng. J., Mar. 1969, pp. 13–20.

du Noüy, P.L., 1919. A new apparatus for measuring surface tension. J. Gen. Physiol., 1: 521–524.

Fatt, I. and Klikoff, W.A., 1959. Effect of fractional wettability on multiphase flow through porous media. Trans., AIME (Am. Inst. Min. Metall. Eng.), 216: 426–432.

Gimatudinov, Sh.K., 1963. The nature of the surface of minerals of oil-bearing rocks. Izv. Vyssh. Uchebn. Zaved., Neft Gaz, 6(7): 37–42 (English translation available from Associated Technical Services, Translation No. 23R75R).

Hassanizadeh, S.M. and Gray, W.G., 1993. Thermodynamic basis of capillary pressure in porous media. Water Resour. Res., 29: 3389–3405.

Hiemenz, P.C., 1986. Principles of Colloid and Surface Chemistry. Marcel Dekker, New York, NY.

Iwankow, E.N., 1960. A correlation of interstitial water saturation and heterogeneous wettability. Prod. Mon. Oct. 24, 1960, No. 12, pp. 18–26.

Klute, A., 1986. Water retention: Laboratory methods. In: A. Klute (Editor), Methods of Soil Analysis, Part 1: Physical and Mineralogical Methods. ASA–SSSA (Am. Soc. Agron.–Soil Sci. Soc. Am.), Madison, WI, pp. 635–662.

Lenhard, R.J. and Parker, J.C., 1988. Experimental validation of the theory of extending two-phase saturation–pressure relations to three-fluid phase systems for monotonic drainage paths. Water Resour. Res., 24: 373–380.

Letey, J., Osborn, J.F. and Valoras, N., 1975. Soil water repellency and the use of nonionic surfactants. Calif. Water Resour. Cent., Davis, CA, Contrib. No. 154.

Leverett, M.C., 1941. Capillary behavior in porous solids. Trans. AIME (Am. Inst. Min. Metall. Eng.), 142: 152–169.

Marquardt, D.W., 1963. An algorithm for least-squares estimation of nonlinear parameters. J. Soc. Ind. Appl. Math., 11: 431–441.

Morrow, N.R., 1975. The effects of surface roughness on contact angle with special reference to petroleum recovery. J. Can. Pet. Technol., Oct.–Dec. 1975, pp. 42–53.

Morrow, N.R., 1976. Capillary pressure correlations for uniformly wetted porous media. J. Can. Pet. Technol., Oct.–Dec. 1976, pp. 49–69.

Powers, S.E. and Tambin, M.E., 1993. Porous media wettability after exposure to complex NAPLs. Eos (Trans. Am. Geophys. Union), 74: 275 (abstract).

Purcell, W.R., 1950. Interpretation of capillary pressure data. Trans. AIME (Am. Inst. Min. Metall. Eng.), 189: 369–371.

Salathiel, R.A., 1973. Oil recovery by surface film drainage in mixed wettability rocks. J. Pet. Technol., Oct. 1973, pp. 1216–1224.

Sharma, M.M. and Wunderlich, R.W., 1985. The alteration of rock properties due to interactions with drilling fluid components. SPE (Soc. Pet. Eng.) Annu. Tech. Conf. Exhibit., Las Vegas, NV, SPE Pap. No. 14302.

Soil Survey Staff, 1975. Soil taxonomy: A basic system of soil classification for making and interpreting soil surveys. USDA–SCS (U.S. Dep. Agric.–Soil Conserv. Serv.) Agric. Handbk. 436, U.S. Gov. Print. Off., Washington, DC.

Stonestrom, D.A. and Rubin, J., 1989. Water content dependence of trapped air in two soils. Water Resour. Res., 25: 1947–1958.

van Genuchten, M.Th., 1980. A closed form equation for predicting the hydraulic conductivity of unsaturated soils. Soil Sci. Soc. Am. J., 44: 892–898.

Wei, M., Bowman, R.S., Wilson, J.L. and Morrow, N.R., 1993. Wetting properties of silane-treated glass exposed to water, air, and oil. J. Colloid Interface Sci., 157: 154–159.